Evaluation of the applicability of an energy method to calculate the damping in a lab-scale structure

Gómez, S. S.; Metrikine, A.

DOI
10.1016/j.proeng.2017.09.018

Publication date
2017

Document Version
Final published version

Published in
X International Conference on Structural Dynamics, EURODYN 2017

Citation (APA)
Gómez, S. S., & Metrikine, A. (2017). Evaluation of the applicability of an energy method to calculate the damping in a lab-scale structure. In F. Vestroni, V. Gattulli, & F. Romeo (Eds.), *X International Conference on Structural Dynamics, EURODYN 2017* (Vol. 199, pp. 459-464). (Procedia Engineering; Vol. 199). Elsevier. https://doi.org/10.1016/j.proeng.2017.09.018

Available online at www.sciencedirect.com

ScienceDirect

Procedia Engineering 199 (2017) 459–464

Procedia Engineering

www.elsevier.com/locate/procedia

X International Conference on Structural Dynamics, EURODYN 2017

Evaluation of the applicability of an energy method to calculate the damping in a lab-scale structure

S. S. Gómez[a,b], A. Metrekine[a]

[a] Faculty of Civil Engineering and Geosciences, Stevinweg 1, 2628CN Delft, The Netherlands
[b] TNO Structural dynamics, Van Mourik Broekmanweg 6, 2628XE Delft, The Netherlands

Abstract

The aim of this paper is to identify the local energy dissipation in a lab-scale structure by means of the energy flow analysis. In most of the existing approaches the damping is identified either in terms of the modal damping factors or at the material scale. In this paper, an alternative method to these global and material-based approaches by studying the energy flow around a certain part of the structure is proposed.

The approach presented in this paper accounts for the energy flow through specific boundaries that surround the structural part of interest. Within this approach, the local energy dissipation can be calculated by isolating specific parts of the structure while taking into account the rest of the structure by means of the energy flux thorough the boundaries. This approach allows to identify both the total energy dissipation and the specific damping operator in the chosen part of the structure.

Keywords: Energy flow, Damping operator, Lab-scale structure, identification;

1. Introduction

The energy dissipation of a mechanical system governs the overall dynamic behaviour. It is, therefore, a topic of great interest in the field of structural dynamics. The energy dissipation in structures is commonly referred to as damping. Although there is a great deal of work in the field of identification [1,2], damping in structures can become difficult to identify and quantify due to its complex nature. Current identification techniques give a damping value associated with a specific frequency for the whole system. If the energy dissipated at specific location is to be studied a large amount of modes need to be involve. This cannot be controlled in structures subjected to environmental loads such as wind. For instance if a structure is excited by wind loads, only the modes that wind is able to excite due to its frequency content will be measurable. This means that, as a rule, an insufficient amount of modes can be measured in order to accurately represent the energy dissipation at a specific location of the structure.

* Corresponding author. Tel.: +31-612-68-7327;
E-mail address: sergio.sanchezgomez@tno.nl, A.Metrikine@tudelft.nl.

10.1016/j.proeng.2017.09.018

In order to overcome this problem an alternative method, based on an energy flow analysis [3-11], is presented in this paper. In order to test this method a lab-scale building structure has been used. The energy dissipation in the joints is studied. Several joints were instrumented to measure both strains and accelerations. The obtained data were used to compute the energy flux in the vicinity of the joints. Finally, assuming various models for the local dissipation, the damping in the joints was analyzed.

2. Experimental work

2.1. Lab-scale building structure and instrumentation

The lab-scale building structure consists of a steel frame with concrete slabs that represent the different floors as shown in Fig. 1. Each of the concrete slabs is supported by four L-shape steel beams. the L-shape beams have a plate welded at both ends that connect the floors (the concrete slab and the L-shape beams) to the L-shape steel columns of the structure making use of bolts. The geometric characteristics of the structure are described in Table 1.

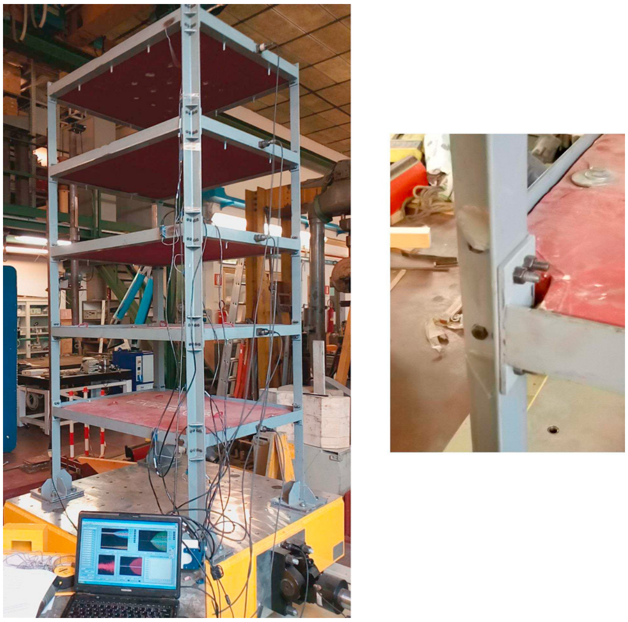

Fig. 1. (a) Lab-scale structure with first instrumentation configuration; (b) Bolted joint.

Table 1. Lab-scale structure characteristics

Height[m]	Width[m]	Depth[m]	ω_1[rad/s]	ξ_1[%]
2.5	1.2	0.9	28.1	1.22

The lab-scale structure is instrumented making use of eight strain gauges glued in one of the columns of the structure in the vicinity of the bolted connection, five accelerometers and one displacement sensor located at the top floor of the structure. In the first instrumentation configuration, the accelerometers are placed on the L-shape steel beams that support the concrete slabs at each floor (Fig. 1), in order to measure the acceleration in the weak direction (horizontal). Thereafter, in the second instrumentation configuration the accelerometers are moved and placed in the columns at the same position as the strain gauges in order to compute the energy flow at each location as shown in Fig. 2.

Fig. 2. Second instrumentation configuration for the energy flow analysis

2.2. Frequency response of the lab-scale structure to a hammer impact

The lab-scale building structure is excited making use of a hammer impact at the top floor. The tip of impact hammer is instrumented with a load cell that measures the force applied to the structure. The frequency content of the force applied to the structure by the impact is shown in Fig. 3.

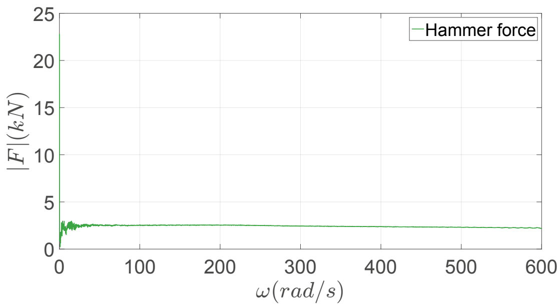

Fig. 3. Frequency spectrum of the hammer force

The energy introduced to the structure by the impact enables us to excite the modes of the structure that are within the spectrum of the hammer induced load. The time signal recorded with each accelerometer using the first instrumentation configuration after the hammer impact is transformed to the frequency domain. Now, the signal is separated to the real and imaginary parts as shown in Fig. 4.

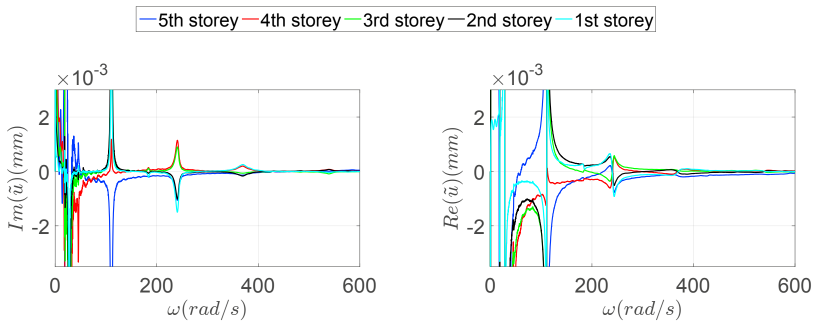

Fig. 4. Frequency response (a) Real part; (b) Imaginary part.

Using the data depicted in Fig. 4(a) the first five natural frequencies ω_N as well as the overall stiffness of the structure can be identified. The values of these frequencies are presented in Table. 2

Table 2. First five natural frequencies of the lab-scale structure

ω_{N_1} [rad/s]	ω_{N_2} [rad/s]	ω_{N_3} [rad/s]	ω_{N_4} [rad/s]	ω_{N_5} [rad/s]
28.1	111	240	366.9	544.2

3. Energy flow formulation

It is assumed that the vibrational energy dissipation is primarily in the joints of the lab-scale structure. This dissipated energy is investigated by means of an energy flow analysis around the joints of each floor separately. To this end, the model depicted in Fig. 5 which accounts for the elements that directly influence the dynamics of the joints, is used.

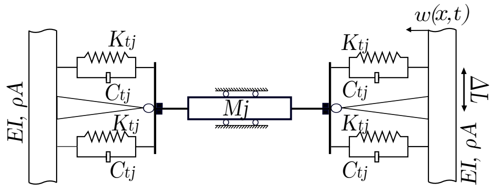

Fig. 5. Segments of Euler-Bernoulli beams with visco-elastic elements representing one floor of the lab-scale structure

The bolted connections are assumed to be fully rigid. Therefore, horizontal displacement of the mass M_j that represents the floor slab is the same as that of the adjacent segments of the columns. A joint of the lab-scale structure is represented by means of springs K_{tj} which mimic the elastic resistance and dashpots C_{tj} which account for the energy dissipation due to the rotational deformation.

An easy way to formulate the energy equation is by multiplying the equation of motion of a floor segment as depicted in Fig. 5 by the velocity and integrated as follows:

$$\begin{aligned}&\int_{\Delta x_j-\Delta L}^{\Delta x_j+\Delta L} \frac{\partial w(x,t)}{\partial t} \left\{ 2\rho A \frac{\partial^2 w(x,t)}{\partial t^2} + 2EI \frac{\partial^4 w(x,t)}{\partial x^4} = -\sum_{j=1}^{N_{stories}} 2\left(K_{t_j} + C_{t_j}\frac{\partial}{\partial t}\right)\right.\\ &\left(\delta\left(x-\Delta x_j-\Delta L\right)\left(w(x,t)-w(\Delta x_j,t)\right) + \delta\left(x-\Delta x_j+\Delta L\right)\left(w(x,t)-w(\Delta x_j,t)\right)\right)\\ &\left.-\delta(x-\Delta x_j)M_j\frac{\partial^2 w(x,t)}{\partial t^2}\right\}\end{aligned} \quad (1)$$

The stiffnesses K_{tj} are identified by setting the dashpots C_{tj} of the equation of motion Eq. 1 to zero and tuning K_{tj} such that the first five natural frequencies match the identified natural frequencies ω_N.

On the other hand, the energy variation equation can be written as:

$$\frac{\partial E_j(t)}{\partial t} + S(x,t)\Big|_{\Delta x_j-\Delta L}^{\Delta x_j+\Delta L} = W_{Diss_j}(t) \quad (2)$$

where,

$$E_j(t) = \frac{1}{2}\left(M_j\left(\frac{\partial w(\Delta x_j,t)}{\partial t}\right)^2 + 2K_{t_j}2\Delta L^2\left(\frac{\partial w(\Delta x_j,t)}{\partial x}\right)^2\right) + E_{j_{beam}}(t) \quad (3)$$

and the $E_{j_{beam}}(x,t)$ can be express as,

$$E_{j_{beam}}(t) = \int_{\Delta x_j-\Delta L}^{\Delta x_j+\Delta L} \frac{1}{2}\left(2\rho A\left(\frac{\partial w(x,t)}{\partial t}\right)^2 + 2EI\left(\frac{\partial^2 w(x,t)}{\partial x^2}\right)^2\right)dx. \quad (4)$$

The $E_j(t)$ is the total energy of the considered structural segment. The energy flux that crosses the boundaries of the segment located at $x = \Delta x_j \pm \Delta L$ is calculated as follows:

$$S(x,t) = 2EI\left(\frac{\partial^2 w(x,t)}{\partial x^2}\frac{\partial^2 w(x,t)}{\partial x \partial t} - \frac{\partial^3 w(x,t)}{\partial x^3}\frac{\partial w(x,t)}{\partial t}\right) \quad (5)$$

where Δx_j is the distance between the bottom of the structure and the position of the mass M_j and W_{Diss_j} is the energy dissipated in the chosen segment.

4. Evaluation of the damping operators based on the energy dissipation

In order to identify a damping operator that reproduces the energy dissipation of the lab-scale structure after a hammer impact test most closely, it is convenient to compute the cumulative energy of each floor over a time window T. To this end, Eq. 2 is integrated over time as follows:

$$E_j(t)|_{t_0}^{t_0+T} + \int_{t_0}^{t_0+T} S(t,x)|_{\Delta x_j-\Delta L}^{\Delta x_j+\Delta L} dt = \int_{t_0}^{t_0+T} W_{Diss_j}(t)dt \tag{6}$$

The left hand side of Eq. 6 is computed making use measurements in the vicinity of the joints, therefore, a value that conforms to the measurements of the energy at each floor is obtained. The energy dissipation W_{Diss_j} is a function that can be represented by a variety of damping operators. In order to evaluate the applicability of the presented method to identify damping, three damping operators namely those of the type $\dot{w}, \frac{\dot{w}}{|\dot{w}|}$ and $\dot{w}|\dot{w}|$ are studied by means of the substitution into the energy dissipation function W_{Diss_j} as follows,

$$W_{Diss_j}(t) = 2C_{tj} \int_{t0}^{t0+T} dt \int_{\Delta x_j-\Delta L}^{\Delta x_j+\Delta L} G_m(t) \frac{\partial w(x,t)}{\partial t} dx \qquad for \quad m = 1,2,3. \tag{7}$$

where,

$$G_1(t) = \left(\delta\left(x-\Delta x_j-\Delta L\right)\left(\frac{\partial w(x,t)}{\partial t} - \frac{\partial w(\Delta x_j)}{\partial t}\right) + \delta\left(x-\Delta x_j+\Delta L\right)\left(\frac{\partial w(x,t)}{\partial t} - \frac{\partial w(\Delta x_j)}{\partial t}\right)\right) \tag{8}$$

$$G_2(t) = \left(\delta\left(x-\Delta x_j-\Delta L\right)\frac{\left(\frac{\partial w(x,t)}{\partial t} - \frac{\partial w(\Delta x_j)}{\partial t}\right)}{\left(|\frac{\partial w(x,t)}{\partial t}|-|\frac{\partial w(\Delta x_j)}{\partial t}|\right)} + \delta\left(x-\Delta x_j+\Delta L\right)\frac{\left(\frac{\partial w(x,t)}{\partial t} - \frac{\partial w(\Delta x_j)}{\partial t}\right)}{\left(|\frac{\partial w(x,t)}{\partial t}|-|\frac{\partial w(\Delta x_j)}{\partial t}|\right)}\right) \tag{9}$$

$$\begin{aligned} G_3(t) = \ &\left(\delta\left(x-\Delta x_j-\Delta L\right)\left(\frac{\partial w(x,t)}{\partial t} - \frac{\partial w(\Delta x_j)}{\partial t}\right)\left(|\frac{\partial w(x,t)}{\partial t}| - |\frac{\partial w(\Delta x_j)}{\partial t}|\right) + \right. \\ &\left. \delta\left(x-\Delta x_j+\Delta L\right)\left(\frac{\partial w(x,t)}{\partial t} - \frac{\partial w(\Delta x_j)}{\partial t}\right)\left(|\frac{\partial w(x,t)}{\partial t}| - |\frac{\partial w(\Delta x_j)}{\partial t}|\right)\right) \end{aligned} \tag{10}$$

The first damping operator G_1 is a conventional viscous damping operator. The second damping operator G_2 is of hysteretic type and the third one G_3 is a quadratic damping operator.

5. Results

In this section the performance of the proposed damping operators is studied by means of comparison of the energy dissipation W_{Diss_j} with the measured energy variation. The comparison is carried out in the frequency domain, therefore, Eq. 6 is transformed to the frequency domain as follows:

$$\begin{aligned} &\sum_{i=1}^{N-1} \left\{E_j(t)|_{t_0}^{t_0+T} + \int_{t_0}^{t_0+T} +S(t,x)|_{\Delta x_j-\Delta L}^{\Delta x_j+\Delta L} dt\right\} e^{\frac{-2\pi ikn}{N}} = \\ &\sum_{i=1}^{N-1} \left\{\int_{t_0}^{t_0+T} W_{Diss_j}(t)dt\right\} e^{\frac{-2\pi ikn}{N}} \qquad k \in \mathbb{Z}, n \in [0, N-1], \end{aligned} \tag{11}$$

where, N is the number of time samples, n is the current sample, k is the current frequency. The energy dissipation obtained with each of the presented damping operators (Eqs. 7-10) is compared to the computed total energy (the left hand side of Eq. 11) per floor. The frequency range used for the comparison encompasses the first five natural frequencies ω_N of the lab-scale building structure. The coefficient C_{tj} of each damping operator is the best fit for each damping operator obtained after the evaluation of Eq. 6. By using the damping coefficient C_{tj} the right hand side of Eq. 11 can be computed and plotted versus frequency.

Fig. 6 illustrates the performance of the damping operators for each floor. The solid lines represent the left-hand side of Eq. 11, which is computed based on the measurements. The other lines represent the right-hand side of Eq. 11 for the three damping operators. Although the damping operators used in this study predict the energy dissipation reasonable well, none of them has a perfect agreement with the frequency dependence expected based on the measurements (solid lines) except for the linear viscous damping at the top floor. This suggests that the damping coefficients C_{tj} may be expected to be frequency dependent even in the case of the assumed nonlinear damping operators.

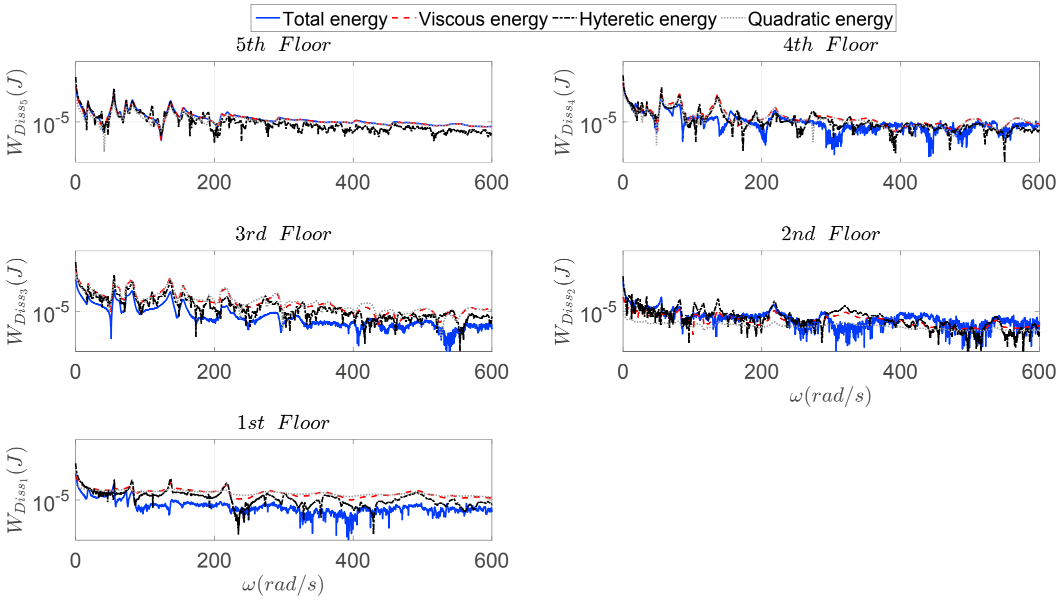

Fig. 6. Comparison of the energy dissipation of the different damping operators at each floor segment

6. Conclusion

In this paper a method to assess the performance of several damping operators is presented. The assessment is done by means of the energy flow analysis around the bolted joints of a lab-scale building structure. The presented approach allows us to study parts of the structure separately, accounting for the rest of the system making use of the energy flow analysis. In this study the lab-scale structure has been excited by means of a hammer impact test. Several damping operators were checked for their ability to reproduce the energy dissipation of the structure as accurately as possible. It has been found that all proposed damping operators give comparable results, although the linear viscous damping operator reproduces the overall energy dissipation more accurately, especially at the top floor segment of the structure.

References

[1] B. Peeters and G. De Roeck, Stochastic system identification for operational modal analysis: A review, ASME Journal of Dynamic systems, Measurement and Control, 123(4):659-667 (2001).

[2] Jimin He and Zhi-Fang Fu, Modal Analysis, (2001), Butterworth-Heinemann.

[3] J .C. Wohlever and R.J. Bernhard, Mechanical energy flow models of rods and beams, Journal of Sound and Vibration, 153 1 1- 19 (1992).

[4] Y. Lase and M.N. Ichchou and L. Jezequel, ENERGY FLOW ANALYSIS OF BARS AND BEAMS: THEORETICAL FORMULATIONS, Journal of Sound and Vibration, 192 1 281 - 305 (1996).

[5] O.M. Bouthier and R.J. Bernhard, Simple models of the energetics of transversely vibrating plates, Journal of Sound and Vibration, 182 1 149 - 164 (1995).

[6] F. Han and R.J. Bernhard and L.G. Mongeau, ENERGY FLOW ANALYSIS OF VIBRATING BEAMS AND PLATES FOR DISCRETE RANDOM EXCITATIONS, Journal of Sound and Vibration, 208 5 841 - 859 (1997).

[7] A. Lebot and L. Jezequel, Energy Methods applied to transverse vibrations of BEAMS, Proceedings of the 4th International Congress on Intensity Techniques, 1993 371-378 Senlis (France).

[8] R.J. Pinnington and D. Lednik, TRANSIENT ENERGY FLOW BETWEEN TWO COUPLED BEAMS, Journal of Sound and Vibration, 1996 189 2 265 - 287.

[9] KS Alfredsson, Active and Reactive Structural Energy Flow, ASME. J. Vib. Acoust. 1997 119(1) 70-79.

[10] S.V. Sorokin and J.B. Nielsen and N. Olhoff, Analysis and optimization of energy flows in structures composed of beam elements – Part I: problem formulation and solution technique, Structural and Multidisciplinary Optimization, 22 1 3–11 (20001).

[11] O.M. Bouthier and R.J. Bernhard, Simple models of energy flow in vibrating membranes, Journal of Sound and Vibration, 182 1 129 - 147 (1995).